IOSR Journal of Applied Physics (IOSR-JAP)
e-ISSN: 2278-4861.Volume 14, Issue 3 Ser. II (May. – June. 2022), PP 25-34
www.iosrjournals.org

AC conductivity and dielectric measurements of bulk Coumarin-6

Mostafa Saad Ebied[1*], Mohammed Nassary[2], Mahmoud Dongol[1]
[1] *Nano and Thin film lab. Physics Department, Faculty of Science, South Valley University, Qena 83523, Egypt*
[2] *Physics Department, Faculty of Science, South Valley University, Qena 83523, Egypt*
**Corresponding author e-mail: Mostafa_saad@sci.svu.edu.eg (M.S. Ebied)*

Abstract
AC conductivity and the related dielectric properties of bulk Coumarian-6 (C6) dye have been investigated as a function of temperature in the 303–403 K temperature regime and 50 Hz to 1 MHz frequency regime. The frequency dependence of AC conductivity follows the Jonscher universal dynamic law $\sigma_{ac}(\omega) = A\omega^{s}$. *The change of the frequency exponent (s) with temperature was analyzed in terms of different conduction mechanisms; It is found that the correlated barrier hopping (CBH) model is the dominant conduction mechanism. The behavior of* $\sigma_{ac}(\omega)$ *increases with increasing temperature and frequency. It has been found that AC activation energy decreases with increasing frequency. The frequency dependence of the dielectric constant (ε') and dielectric loss (ε") for bulk C6 has been studied using the complex permittivity. It is found that ε' and ε" are decreases with increasing frequency and increases with temperature. The dielectric modulus shows the non-Debye relaxation in the material. The extracted relaxation time by using the imaginary part of modulus (M") is found to follow the Arrhenius law.*

Key words: *Coumarin; Ac Conductivity; Dielectric properties; organic semiconductor.*

Date of Submission: 06-06-2022 Date of Acceptance: 21-06-2022

I. Introduction

Organic semiconductors (OSCs) are known as organic π-conjugated materials with good charge transport and/or electroluminescent properties, and widely used in organic and hybrid electronic devices such as organic light emitting diodes (OLEDs), organic photovoltaic cells (OPVs) and organic field-effect transistors (OFETs)[1]. Coumarin and its derivatives have received a considerable interest in industry in the form of dye lasers and high-efficiency dye-sensitized solar cells due to their interesting and promising optical features, such as fluorescence in visible light, significant Stokes shifts, high quantum yields, and solubility [2]. Coumarin-6 (C6) molecular crystal possesses a relatively high melting point around 220 °C, a high surface morphology stability, and an efficient light emission, making it an important organic material for optoelectronic devices[3]. The understanding of the charge transport mechanism in the organic semiconductors materials is very important both from fundamental and technological point of view. We can get some information about transport mechanism form conductivity measurements such as DC and AC conductivity measurements. DC conductivity provide an idea about the conduction of free charges under the application of an external electric field, while the AC measurements are often used to investigate the behavior of such low mobility compounds and one can obtain information about the dielectric constant, the loss tangent, the mechanism of conduction and the activation energy from AC measurements[4]. The advantage of AC measurements over the DC measurements is that the internal time dependent processes in the insulator can be investigated with AC measurements. Moreover, the AC voltage bias never exceeds a few hundred millivolts; thus, the maximum field within the sample is kept to a minimum and there is little danger of more than one conduction process being active[5,6]. Various models such as Quantum-Mechanical Tunneling (QMT) model[7], Small Polaron Tunneling (SPT) model[8], Large Polaron Tunneling (LPT) model[8], Atomic Hopping (AH) model and Correlated Barrier Hopping (CBH) model[9] have been proposed to explain the AC conductivity. The present work focuses on the effects of temperature (303 K–403 K) and applied frequencies (50 Hz–1 MHz) on the electrical conductivity of bulk Coumarin-6 respectively. Moreover, dielectric constants and complex dielectric modulus of bulk Coumarin-6 are also studied.

II. Experimental Methods

For AC measurements, two conducting layers of silver were deposited onto both surfaces of C6 disc to behave as ohmic contacts. The temperature of the sample was recorded during the electrical measurements by using Chromel-Alumel thermocouple with an accuracy of ±1 K. All measurements were performed at different temperatures in air and under dark conditions. The AC parameters such as the impedance, Z capacitance, C and dissipation factor, tan δ were measured using programmable automatic LCR Bridge (model Hioki 3536). The measurements were performed in the temperature and frequency ranges of (303 - 403 K) and (50 Hz - 1 MHz), respectively.

III. Results and Discussion

3.1 Ac conductivity

AC conductivity and dielectric relaxation have been proven to be a significant procedure for studying the relaxation and conduction mechanisms in organic materials. The frequency dependence of the electrical conductivity offers important information on the relaxation of charge carriers in the materials. The crucial features of the charge carriers' dynamics may, therefore, be deduced from the AC conductivity measurement[5]. The total electrical conductivity $\sigma_t(\omega)$ can be calculated using the following equation[10,11]:

$$\sigma_t(\omega) = \sigma_{dc} + \sigma(\omega) \quad (1)$$

Where $\sigma_{dc}$is the direct current (dc) conductivity, which is independent on frequency, while σ_{ac} is the alternating current (ac) conductivity, which varies with frequency. At low frequency, the experimental data of $\sigma_t(\omega)$ can extrapolated to zero frequency (ω=0) to get σ_{dc} values. The values of $\sigma_{ac}(\omega)$ can be obtained by subtracting the dc-conductivity values from the experimental data of the total electrical conductivity $\sigma_t(\omega)$. **Fig. 1** illustrated the frequency dependent ac-electrical conductivity,σ_{ac}, as a function of temperatures.

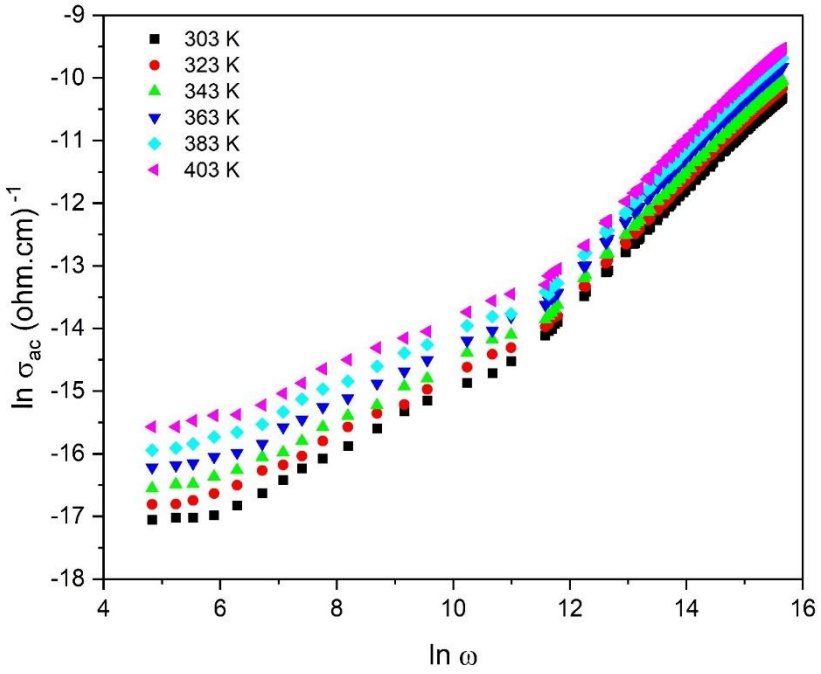

Figure 1:Frequency dependence of σ_{ac} for C6 at different temperatures.

The equation that describes the frequency dependence of ac-electrical conductivity σ_{ac} can be written as follows[4,12]:

$$\sigma_{ac} = A\omega^s \quad (2)$$

Where ω is the angular frequency, A is a constant for a particular temperature, and **s** is the frequency exponent, which is usually less than or equal to one. It is clear from the figure that σ_{ac} increases with increasing frequency according to Eq. (2). The values of s at different temperatures are obtained from the slope of the linear $\ln(\sigma_{ac})$ vs. $\ln(\omega)$. The value and temperature-dependent behavior of **s** determines which conduction mechanism is most suited for the material. Numerous theoretical models have been proposed to understand the conduction mechanism of materials, such as, the quantum-mechanical tunneling (QMT) model, large polaron tunneling (LPT) model, small polaron tunneling (SPT) model and correlated barrier hopping (CBH) model[9]. In each model of the mentioned above, "**s**" depend on temperature and/or frequency in different ways, for example in

QMT model "**s**" is expected to be frequency-dependent but temperature-independent while in LPT model "**s**" has to be temperature and frequency dependent, "**s**" decreases with increasing temperature from unity at room temperature to a minimum value at a certain temperature, then it increases with increasing[13]. In the case of SPT model "**s**" is expected to increase as temperature increases and finally in CBH model, it is expected that "**s**" would decrease with increasing temperature[14].

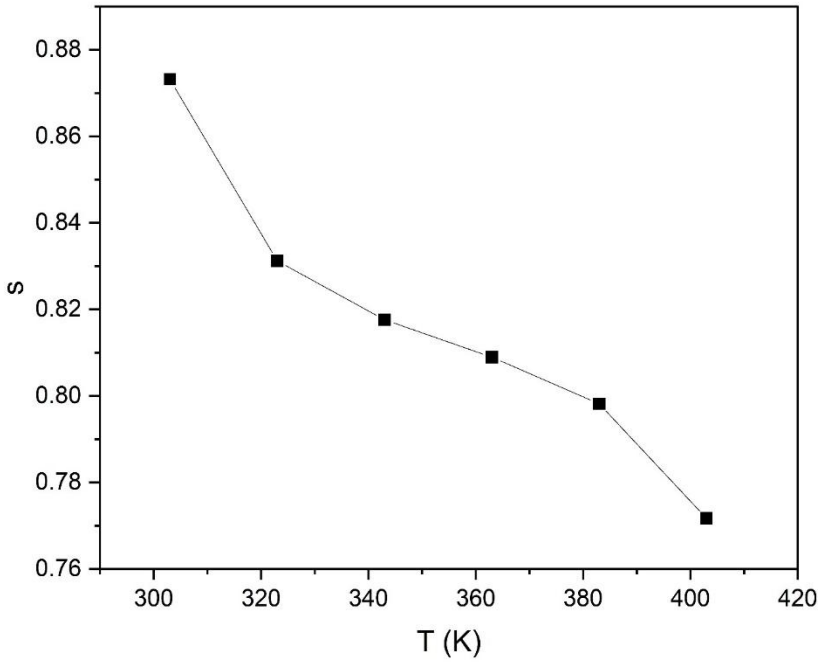

Figure 2:Temperature dependence of power exponent (s).

Fig. 2 shows that the obtained values of **s** for the investigated sample decrease with increasing temperatures, indicating that the conduction mechanism can be explained in terms of correlated barrier hopping model (CBH), in which the frequency exponent **s** is less than one at different temperatures, and decreased with increasing temperature. In CBH model, the charge carriers hop over the potential barrier between two charged defect states and the exponent **s** is given by[8,9]:

$$s = 1 - \frac{6k_B T}{[W_M + k_B T \ln(\omega\tau_0)]} \qquad (3)$$

where k_B is the Boltzmann constant, W_M the maximum barrier height for hopping at infinite inter site separation[15] which is called the binding energy of the carrier in its localized sites[16], and τ_0 the characteristic relaxation time which is in the order of an atom vibrational period($\tau_0=10^{-13}$s)[17]. equation (3) can be approximated to yield the following relation[18]:

$$s = 1 - \frac{6k_B T}{W_M} \qquad \text{III)}$$

W_M can be calculated using the last equation by plotting 1-s versus T, which is shown in **Fig. 3** and its slope is used to calculate the binding energy W_M and it was found to be 0.99049 eV.

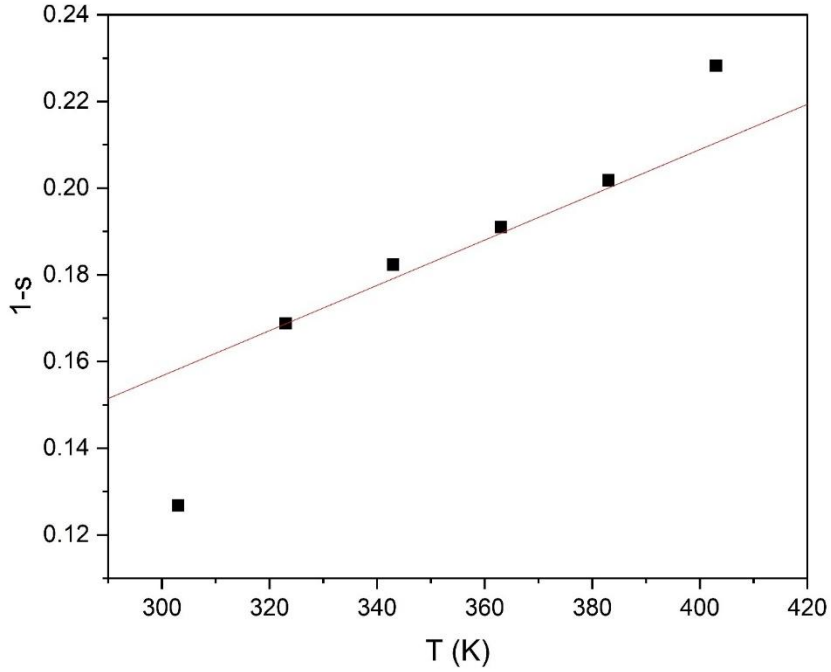

Figure 3:Temperature dependence of 1-s

3.1.1 Temperature dependent conductivity

The temperature dependence of $\sigma_{ac}$of bulk C6 is shown in **Fig. 4** at different frequencies. The ln(σ_{ac}) increases linearly by increasing the temperature. This suggests that the ac conductivity is a thermally activated process for different localized states in the gap[19]. The dependence of ac conductivity,σ_{ac}, on temperature was found to obey the well-known Arrhenius relation[20]:

$$\sigma_{ac} = \sigma_0 \exp(\frac{-\Delta E_{ac}}{k_B T}) \qquad (5)$$

where σ_0 the pre-exponential constant, ΔE_{ac} is the ac-activation energy. The activation energy of ac-conduction for different frequencies was determined from the slope of the obtained straight lines in **Fig. 4**. The frequency dependence of the ΔE_{ac} is shown in **Fig. 5**. It is clear that ΔE_{ac} tends to decrease with increasing applied frequency. Such a decrease can be attributed to the contribution of the applied frequency to the conduction mechanism which confirms the hopping conduction to be the dominant mechanism[21]. Thus, the increase of the applied frequency enhances the electronic jumps between the localized states which agree with other workers[22–24].

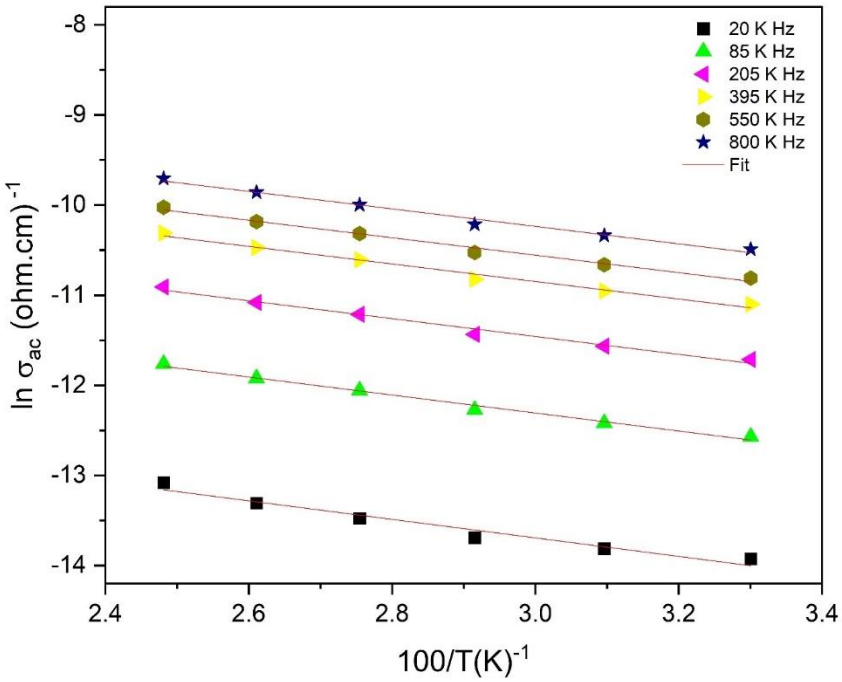

Figure 4:Temperature dependence of σ_{ac} for C6 at different frequencies.

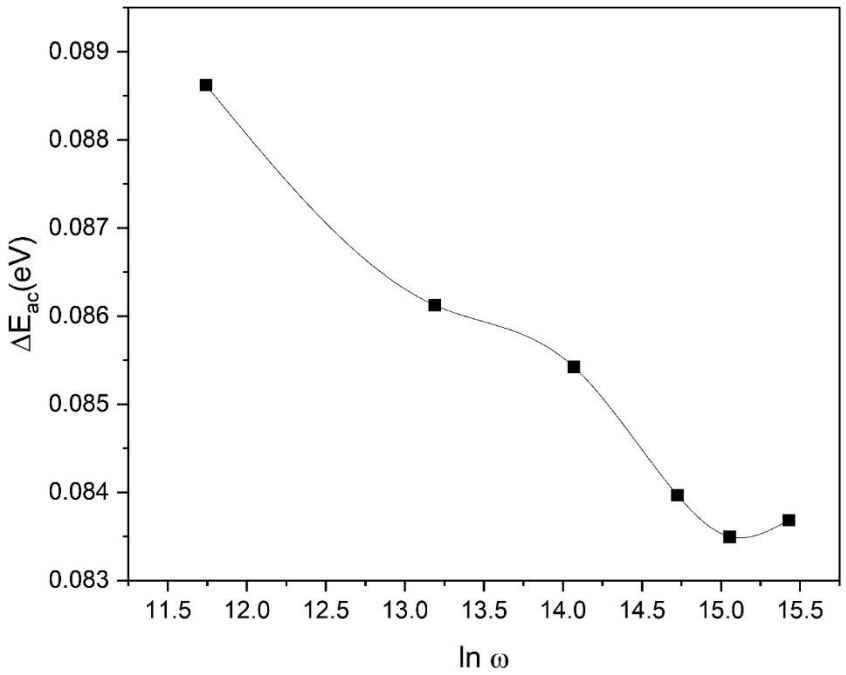

Figure 5:Frequency dependence of the AC activation energy for C6.

3.1.2 Dielectric studies

Dielectric studies are an essential source of valuable information about conduction processes since they can be used to recognize the origin of the dielectric losses, the electrical and dipolar relaxation time and its activation energy[25]. Studying the dielectric properties for the material enriches knowledge about the electric properties as a function of temperature and frequency. Two fundamental electrical characteristics of materials are defined by the dielectric analysis, i.e., (i) the capacitive insulating nature, which represents its ability to store electrical charge, and (ii) the conductive nature, which represents its ability to transfer electric charge[26,27]. The dielectric properties are associated with different kinds of polarization (electronic, ionic, relaxation and space charge)[28,29]. the complex permittivity (ε^*) of the material is given by:

$$\varepsilon^* = \varepsilon_1 + i\,\varepsilon_2 \qquad (6)$$

Where ε_1 and ε_2 are the real and imaginary parts of the complex permittivity. ε_1 is related to the capacitive nature of the material and is a measure of the reversible energy stored in the material by polarization, while ε_2 is a measure of the energy required for molecular motion[30,31], the relation that combines each of them is given by:

$$\varepsilon_2 = \varepsilon_1 \tan\delta \quad (7)$$

Where tan δ (δ = 90- φ) is the loss tangent and φ is the phase angle. The real part of the permittivity (dielectric constant) ε_1 is calculated using the formula:

$$\varepsilon_1 = \frac{C_p d}{\varepsilon_0 A} \quad (8)$$

Where C_p is capacitance of the sample in farad, d is the disk thickness and ε_0=8.854 x 10^{-12} F/ m is the permittivity of free space and A is cross sectional area of the disk. The capacitance (Cp) and loss tangent (tan(δ)) can be obtained directly from the measurements. The dielectric properties measurements were performed in the temperature range from (303– 403 K) and frequency range from (50–10^6 Hz).

Fig. 6 shows the dependence of the dielectric constant, ε_1, on frequency at different temperatures. which illustrates that the dielectric constant ε_1 values decreases with the increase in frequency. This behavior can be explained as follows: at low frequencies, ε_1 for polar materials is due to the contribution of multi-components of polarizability; relaxation polarization (interfacial and orientational) and deformational polarization (ionic and electronic). As the frequency increases, the dipoles will no longer be able to rotate sufficiently rapidly, so their oscillations begin to lag behind the field, further increasing of frequency results in stopping of orientation and dipoles will be completely unable to follow the field, so that the decreasing of ε_1 at a higher frequency approaching a constant value (frequency independent) result from the interfacial polarization[32]. The variation of the dielectric loss, ε_2, with frequencies is presented in **Fig. 7**. ε_2 values are found to follow the same trend as ε_1. Dipole losses, dielectric losses and conduction losses are considered the main origins of the dielectric losses[14].

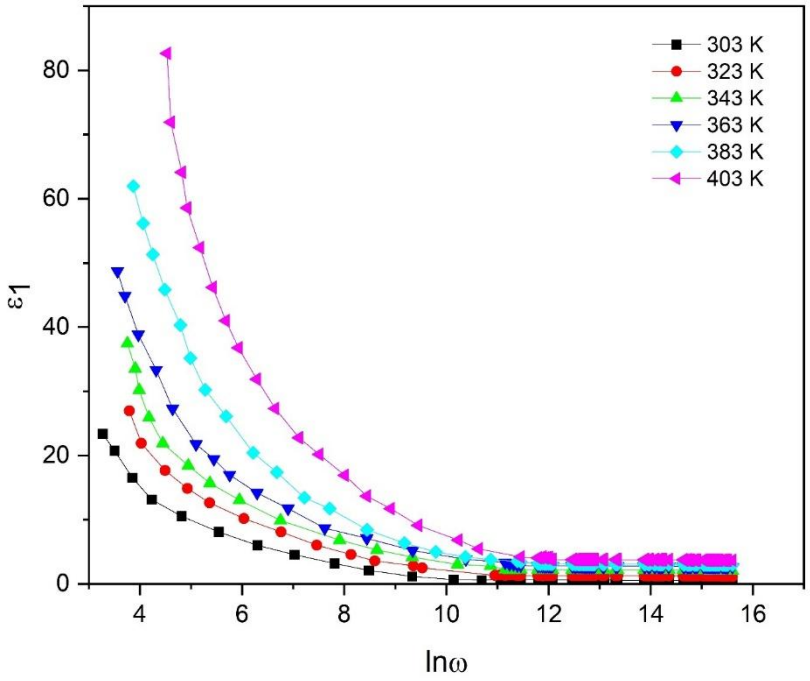

Figure 6:Frequency dependence of dielectric constant, ε_1, for C6 at different temperatures.

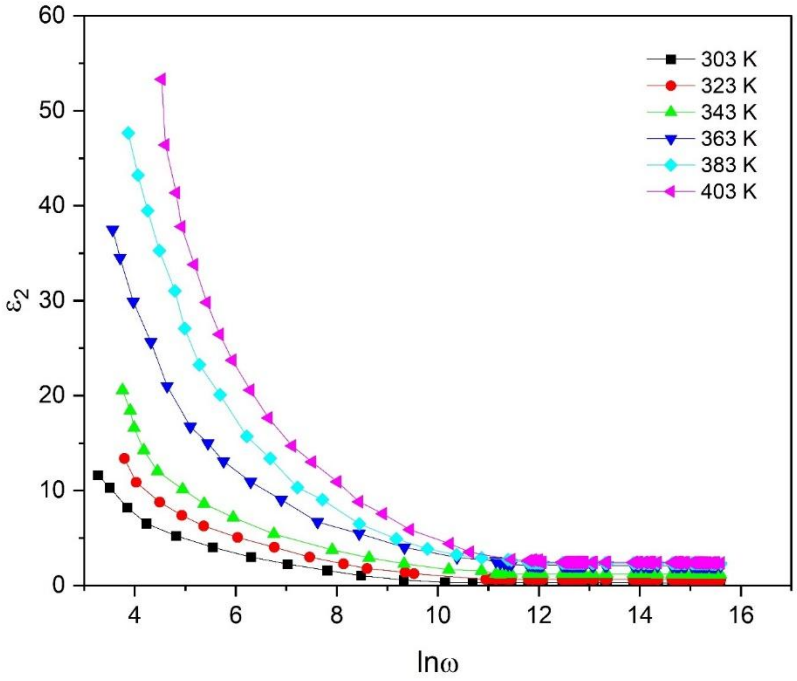

Figure 7:Frequency dependence of, ε_2, for C6 at different temperatures.

3.1.3 Complex dielectric modulus

Electric modulus, M*, can be considered a different representation to express dielectric properties of materials, this alternative formulism may often give a new in-depth vision about electrical and dielectric properties of materials. Comparison between electric modulus, M*, and complex dielectric permittivity, ε*, enables us to distinguish long-range electrical conductivity from local dielectric relaxation (e.g. dipole reorientation)[33]. The unwanted effects of extrinsic relaxations are minimized by the modulus representation. Thus, common difficulties like impurity conduction effects, space charge injection phenomena and electrode nature which appear to obscure relaxation in the permittivity presentation can be ignored[34]. The complex electric modulus is derived from the complex permittivity equation[35]. According to Macedo et al [36], the real and imaginary parts of the electric modulus M' and M'' can be calculated from ε_1 and ε_2 as follows:

$$M^* = \frac{1}{\varepsilon^*} = M' + jM" \tag{9}$$

$$M' = \frac{\varepsilon_1}{\varepsilon_1^2 + \varepsilon_2^2} \tag{10}$$

$$M" = \frac{\varepsilon_2}{\varepsilon_1^2 + \varepsilon_2^2} \tag{11}$$

The obtained modulus $M''$is shown in **Fig. 8**. In the low frequency region, M'' values tend to zero, which confirms the negligible contribution of electrode effects. Therefore, these effects may be ignored [37]. The variation of M'' with frequency shows that the relaxation peaks are moving towards higher frequencies by increasing temperature. This behavior indicates that the dielectric relaxation is thermally activated in which the hopping process of the charge carrier dominates intrinsically. The asymmetric broadening of the M'' peak shows the spread of relaxation with time constant so, relaxation of our sample follows the non-Debye type. The frequency region below peak maximum determines the range in which charge carriers are mobiles on long-range distances.

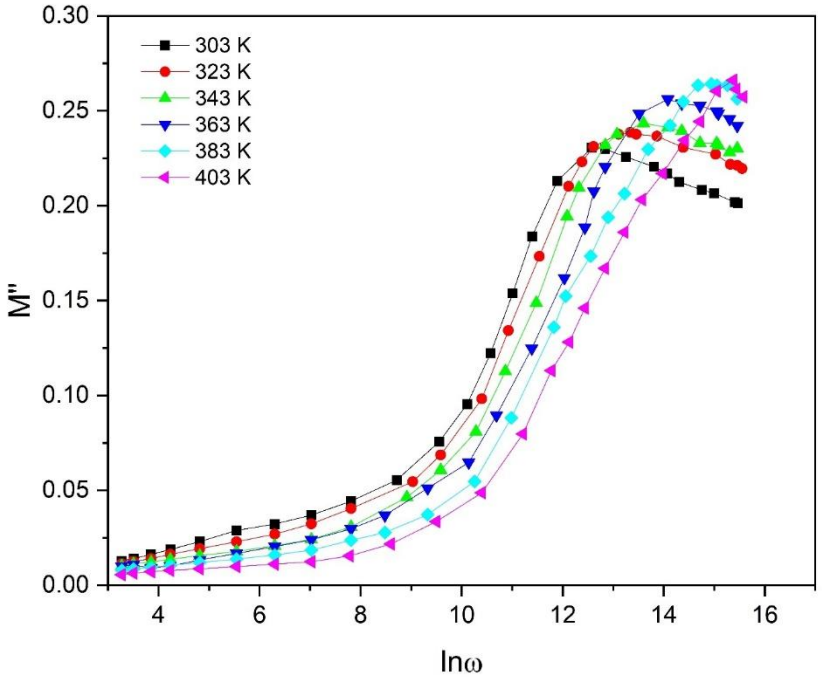

Figure 8:Frequency dependence of electric modulus, M"; for C6at different temperatures.

As a convenient measure of the characteristic relaxation time, one can choose the inverse of frequency of the maximum position, where. $\tau_m = \omega_m^{-1}$. Thus, we can determine the temperature dependence of the characteristic relaxation time as shown in **Fig. 9**, which described by Arrhenius relation[38]:

$$\omega_m = \omega_0 \exp(-\Delta E_\omega / K_B T) \quad (12)$$

where ω_0 the pre-exponent factor, ΔE_ω is the activation energy for dielectric relaxation, which is about 0.288 eV.

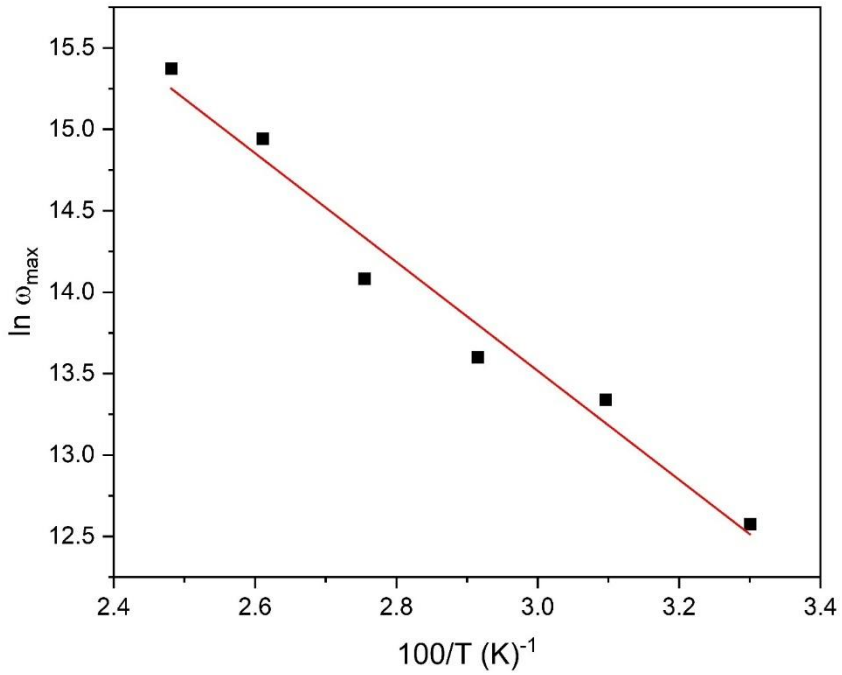

Figure 9:Variation of ln ω_{max} vs. 1000/T for C6.

IV. Conclusion

AC conductivity of bulk material of C6 in a disc form has been studied over a wide range of frequencies and temperatures. Values of frequency exponent factor (s) were found to decrease with increasing temperature. The correlated barrier hopping (CBH) was found to be the suitable conduction mechanism for AC

conductivity. The frequency dependence of ΔE_{ac} was found to decrease with frequency. The behavior of dielectric constant and dielectric loss was found to increase with temperature and decrease with frequency. Electric modulus, M* has been used as a different representation to express dielectric properties of material. Variation of M″ with frequency showed that the relaxation peaks move towards higher frequencies by increasing temperature. The activation energy for dielectric relaxation, ΔE_{ω}, was found about 0.288 eV.

References

[1]. J.C.S. Costa, R.J.S. Taveira, C.F.R.A.C. Lima, A. Mendes, L.M.N.B.F. Santos, Optical band gaps of organic semiconductor materials, Opt. Mater. (Amst). 58 (2016) 51–60. https://doi.org/10.1016/j.optmat.2016.03.041.

[2]. F.A. Mir, U.R. Shakeel, K. Asokan, S.H. Khan, G.M. Bhat, Optical, DC and AC electrical investigations of 4-hydroxy coumarin molecule as an organic Schottky diode, J. Mater. Sci. Mater. Electron. 25 (2014) 1258–1263. https://doi.org/10.1007/s10854-014-1718-4.

[3]. K.L. Chen, H.T. Liu, J.H. Yu, Y.H. Tung, Y.S. Chou, C.C. Yang, J.S. Wang, J.L. Shen, K.C. Chiu, Characterization of coumarin-6 polycrystalline films growth from vacuum deposition at various substrate temperatures, Sci. Rep. 8 (2018) 16740. https://doi.org/10.1038/s41598-018-34813-w.

[4]. A.A.A. Darwish, M.M. El-Nahass, A.E. Bekheet, AC electrical conductivity and dielectric studies on evaporated nanostructured InSe thin films, J. Alloys Compd. 586 (2014) 142–147. https://doi.org/10.1016/j.jallcom.2013.10.054.

[5]. A.A.A. Darwish, A.M. Hassanien, T.A. Hanafy, M.M. El-Nahass, On the nature of bulk electrical relaxation in 4-tricyanovinyl-N,N-diethylaniline (TCVA), Synth. Met. 199 (2015) 339–344. https://doi.org/10.1016/j.synthmet.2014.12.007.

[6]. M.M. El-Nahass, H.S. Metwally, H.E.A. El-Sayed, A.M. Hassanien, Electrical conductivity and dielectric relaxation of bulk iron (III) chloride tetraphenylporphyrin, Mater. Chem. Phys. 133 (2012) 649–654. https://doi.org/10.1016/j.matchemphys.2012.01.042.

[7]. M. Pollak, T.H. Geballe, Low-Frequency Conductivity Due to Hopping Processes in Silicon, Phys. Rev. 122 (1961) 1742–1753. https://doi.org/10.1103/PhysRev.122.1742.

[8]. A.R. Long, Frequency-dependent loss in amorphous semiconductors, Adv. Phys. 31 (1982) 553–637. https://doi.org/10.1080/00018738200101418.

[9]. S.R. Elliott, A theory of a.c. conduction in chalcogenide glasses, Philos. Mag. 36 (1977) 1291–1304. https://doi.org/10.1080/14786437708238517.

[10]. A.K. Jonscher, The 'universal' dielectric response, Nature. 267 (1977) 673–679.

[11]. N.F. Mott, E.A. Davis, Electronic processes in materials, Oxford university press, 1963. https://doi.org/10.1016/0016-0032(63)90430-7.

[12]. A.K. Jonscher, Dielectric relaxation in solids, J. Phys. D. Appl. Phys. 32 (1999) R57. https://doi.org/10.1088/0022-3727/32/14/201.

[13]. M. Pollak, G.E. Pike, Ac conductivity of glasses, Phys. Rev. Lett. 28 (1972) 1449–1451. https://doi.org/10.1103/PhysRevLett.28.1449.

[14]. I.M. Soliman, M.M. El-Nahass, Y. Mansour, Electrical, dielectric and electrochemical measurements of bulk aluminum phthalocyanine chloride (AlPcCl), Solid State Commun. 225 (2016) 17–21. https://doi.org/10.1016/j.ssc.2015.10.011.

[15]. V.K. Bhatnagar, K.L. Bhatia, Frequency dependent electrical transport in bismuth-modified amorphous germanium sulfide semiconductors, J. Non. Cryst. Solids. 119 (1990) 214–231. https://doi.org/10.1016/0022-3093(90)90845-D.

[16]. B.K. Chaudhuri, K. Chaudhuri, K.K. Som, Concentration and frequency dependences of A.C. conductivity and dielectric constant of iron-bismuth oxide glasses-II, J. Phys. Chem. Solids. 50 (1989) 1149–1155. https://doi.org/10.1016/0022-3697(89)90024-3.

[17]. G.E. Pike, Ac Conductivity of Scandium Oxide and a New Hopping Model for Conductivity, Phys. Rev. B. 6 (1972) 1572–1580. https://doi.org/10.1103/PhysRevB.6.1572.

[18]. S.R. Elliott, Temperature dependence of A.C. conductivity of chalcogenide glasses, Philos. Mag. B Phys. Condens. Matter; Stat. Mech. Electron. Opt. Magn. Prop. 37 (1978) 553–560. https://doi.org/10.1080/01418637808226448.

[19]. F. Yakuphanoglu, Y. Aydogdu, U. Schatzschneider, E. Rentschler, DC and AC conductivity and dielectric properties of the metal-radical compound: Aqua[bis(2-dimethylaminomethyl-4-NIT-phenolato)]copper(II), Solid State Commun. 128 (2003) 63–67. https://doi.org/10.1016/S0038-1098(03)00651-3.

[20]. A. Djemal, B. Louati, K. Guidara, Rietveld refinement and electrical properties of cadmium lithium phosphate, J. Mater. Sci. Mater. Electron. 28 (2017) 13806–13813. https://doi.org/10.1007/s10854-017-7226-6.

[21]. E.M. El-Menyawy, H.M. Zeyada, M.M. El-Nahass, AC conductivity and dielectric properties of 2-(2,3-dihydro-1,5-dimethyl-3-oxo-2-phenyl-1H-pyrazol-4-ylimino)-2-(4-nitrophenyl)acetonitrile thin films, Solid State Sci. 12 (2010) 2182–2187. https://doi.org/10.1016/j.solidstatesciences.2010.10.001.

[22]. M.A.M. Seyam, Dielectric relaxation in polycrystalline thin films of In 2 Te 3, Appl. Surf. Sci. 181 (2001) 128–138. https://doi.org/10.1016/S0169-4332(01)00378-6.

[23]. M.M. El-Nahass, H. Kamal, M.H. Elshorbagy, K. Abdel-Hady, Electrical and dielectric properties of chromotrope 2R in pellet and thin film forms, Org. Electron. 14 (2013) 2847–2853. https://doi.org/10.1016/j.orgel.2013.08.010.

[24]. M. Dongol, M.M. El-Nahass, A. El-Denglawey, A.A. Abuelwafa, T. Soga, Alternating current characterization of nano-Pt(II) octaethylporphyrin (PtOEP) thin film as a new organic semiconductor, Chinese Phys. B. 25 (2016). https://doi.org/10.1088/1674-1056/25/6/067201.

[25]. F.I.H. Rhouma, A. Dhahri, J. Dhahri, M.A. Valente, Dielectric, modulus and impedance analysis of lead-free ceramics Ba 0.8La 0.133Ti 1-x Sn x O 3 (x=0.15 and 0.2), Appl. Phys. A Mater. Sci. Process. 108 (2012) 593–600. https://doi.org/10.1007/s00339-012-6935-1.

[26]. I.S. Yahia, N.A. Hegab, A.M. Shakra, A.M. Al-Ribaty, Conduction mechanism and the dielectric relaxation process of a-Se 75Te 25-xGa x (x=0, 5, 10 and 15 at wt%) chalcogenide glasses, Phys. B Condens. Matter. 407 (2012) 2476–2485. https://doi.org/10.1016/j.physb.2012.03.049.

[27]. H.E. Atyia, N.A. Hegab, M.A. Affi, M.I. Ismail, Influence of temperature and frequency on the AC conductivity and dielectric properties for Ge15Se60Bi25 amorphous films, J. Alloys Compd. 574 (2013) 345–353. https://doi.org/10.1016/j.jallcom.2013.04.155.

[28]. K.C. Kao, Dielectric Phenomena in Solids, Elsevier Academic Press, 2004. https://doi.org/10.1016/B978-0-12-396561-5.X5010-5.

[29]. C.A. Harper, Handbook of ceramics, glasses and diamonds, McGraw Hill Professional, 2001.

[30]. H.E. Atyia, Electrical conductivity and dielectric relaxation of bulk Se 70Bi(30 - X)Tex, x = (0, 15) chalcogenide glasses, J. Non. Cryst. Solids. 391 (2014) 83–90. https://doi.org/10.1016/j.jnoncrysol.2014.03.002.

[31]. H.E. Atyia, A.M. Farid, N.A. Hegab, AC conductivity and dielectric properties of amorphous GexSb40-xSe60 thin films, Phys. B Condens. Matter. 403 (2008) 3980–3984. https://doi.org/10.1016/j.physb.2008.07.048.

[32]. B. Tareev, Physics of Dielectric Materials (Moscow: Mir), Mir publishers, 1979.
[33]. P.K. Bajpai, K.N. Singh, Dielectric relaxation and ac conductivity study of Ba(Sr 1/3Nb2/3)O3, Phys. B Condens. Matter. 406 (2011) 1226–1232. https://doi.org/10.1016/j.physb.2010.12.069.
[34]. A. Abu Bakr, A.M. North, G. Kossmehl, Charge carrier hopping in poly(arylene vinylenes), Eur. Polym. J. 13 (1977) 799–803. https://doi.org/10.1016/0014-3057(77)90025-8.
[35]. B.G. Soares, M.E. Leyva, G.M.O. Barra, D. Khastgir, Dielectric behavior of polyaniline synthesized by different techniques, Eur. Polym. J. 42 (2006) 676–686. https://doi.org/10.1016/j.eurpolymj.2005.08.013.
[36]. P.B. Macedo, C.T. Moynihan, R. Bose, Role of Ionic Diffusion in Polarization in Vitreous Ionic Conductors., Phys. Chem. Glas. 13 (1972) 171–179.
[37]. F.S. Howell, R.A. Bose, P.B. Macedo, C.T. Moynihan, Electrical relaxation in a glass-forming molten salt, J. Phys. Chem. 78 (1974) 639–648. https://doi.org/10.1021/j100599a016.
[38]. A.S.A. Khiar, R. Puteh, A.K. Arof, Conductivity studies of a chitosan-based polymer electrolyte, Phys. B Condens. Matter. 373 (2006) 23–27. https://doi.org/10.1016/j.physb.2005.10.104.

Mostafa Saad Ebied, et. al. "AC conductivity and dielectric measurements of bulk Coumarin-6." *IOSR Journal of Applied Physics (IOSR-JAP)*, 14(03), 2022, pp. 25-34.